

28th IAEA Fusion Energy Conference

Summary: Magnetic Fusion Experiments - I

Core Confinement	60
MHD & Stability	26
Energetic Particles	17
Divertor & SOL	42

M.C. Zarnstorff

PPPL, USA

15 May 2021

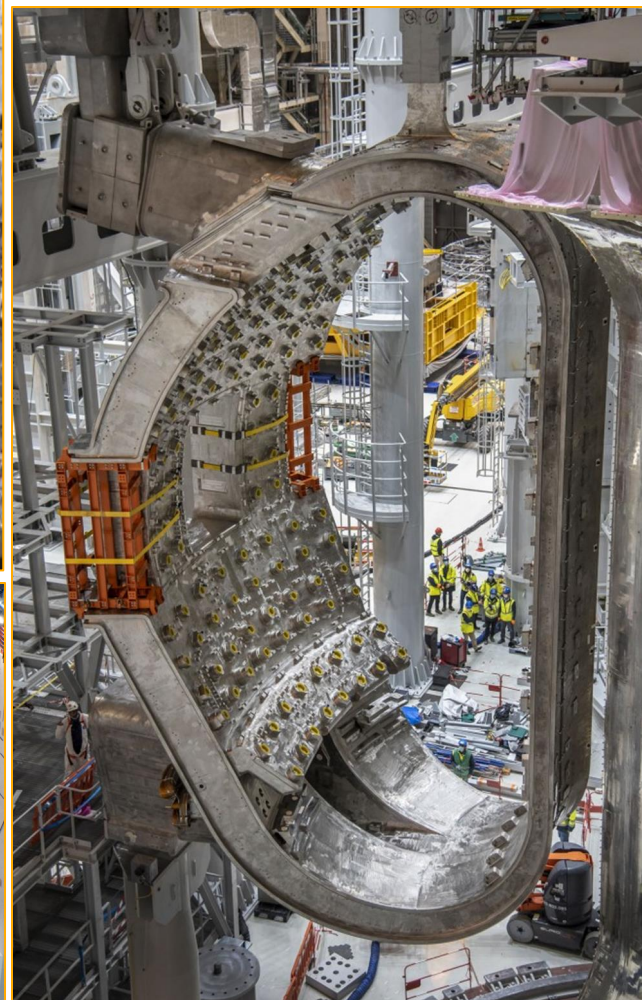
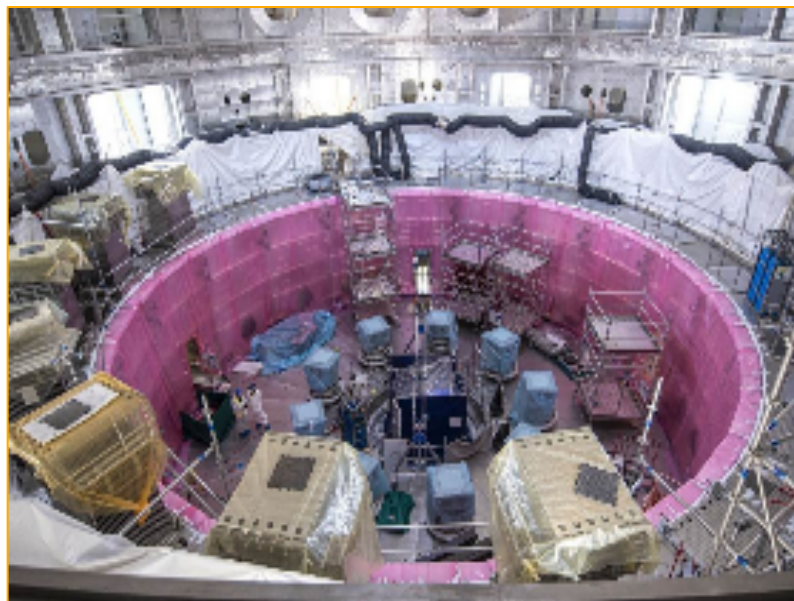
ITER Construction – Fantastic Progress

- Major components being delivered
- First sector starting assembly
- Cryostat & coils being installed in pit
- Buildings & infrastructure being completed
- Incorporation of new developments, e.g. shattered pellets DM
- Research prep. progressing

1st plasma: late 2025

Community support is essential to success.

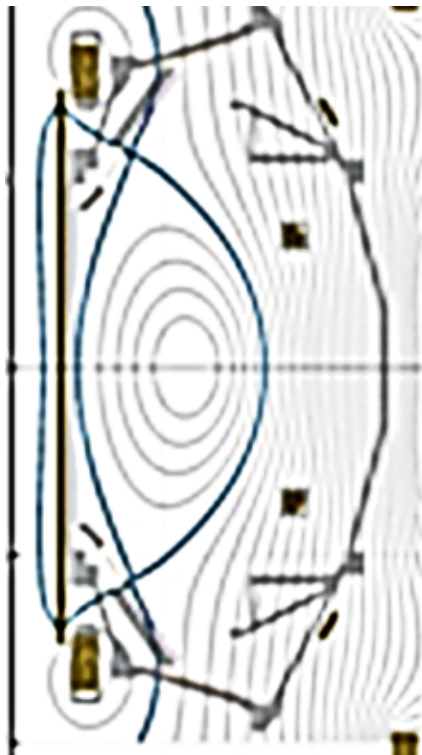
B.Bigot OV/1-1



VV Sector 6 in the sector sub-assembly tool

Installation of the cryostat side-wall and PF-coil #6 in the tokamak pit

New & Upgraded Experiments Operating



ST-40 (Tok. Energy)

$R=0.4-0.6m, A=1.6-1.8$
 $B_T=3T, I_p=2MA$

First plasma: 2019
 ST performance,
 high T

M.Gryaznevich OV/4-5

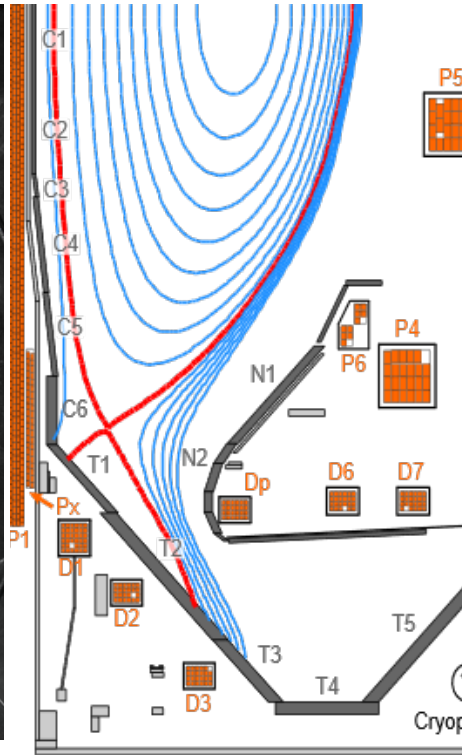


HL-2M (CN)

$R=1.78m, A=2.8$
 $B_T=2.25T, I_p=2.5MA$

First plasma: 2020
 High performance
 w/ adv. divertors

X.Duan EX/4-3



MAST-U (UK)

$R=0.85m, A=1.3$
 $B_T=0.92T, I_p=2MA$

First plasma: 2020
 Super-X Divertor
 ST performance

J.Harrison EX/P6-1538

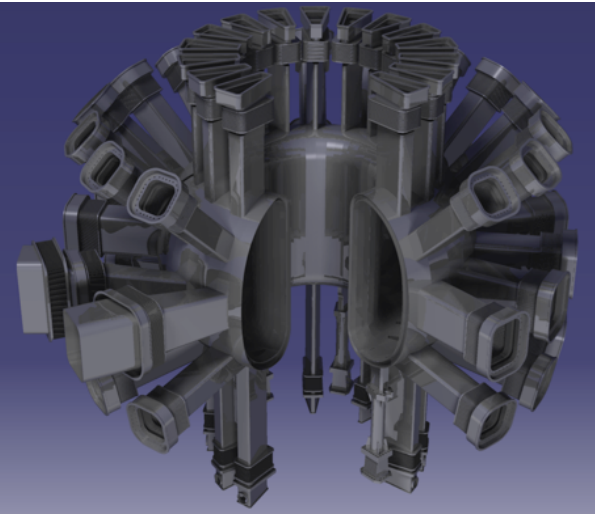


JT60-SA (JP, EU)

$R=3m, A=2.5$
 $B_T=2.25T, I_p=5.5MA$
 Superconducting
 Commissioning
 Long pulse adv.
 scenarios

Y.Kamada OV/2-4

New Experiment Projects/Upgrades

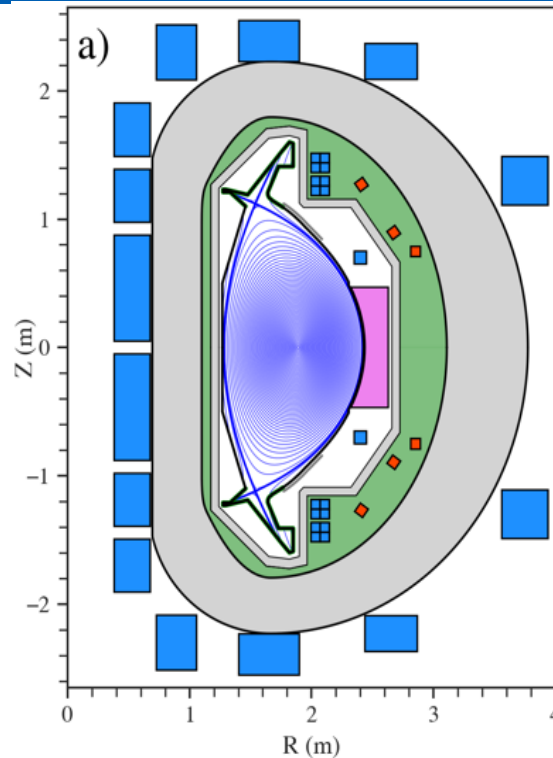


DTT (IT)

$R=2.19\text{m}$, $A=3.1$
 $B_T=6\text{T}$, $I_p=5.5\text{MA}$

Exhaust physics,
core-edge integration
divertor test facility

P.Martin EX/P-1053

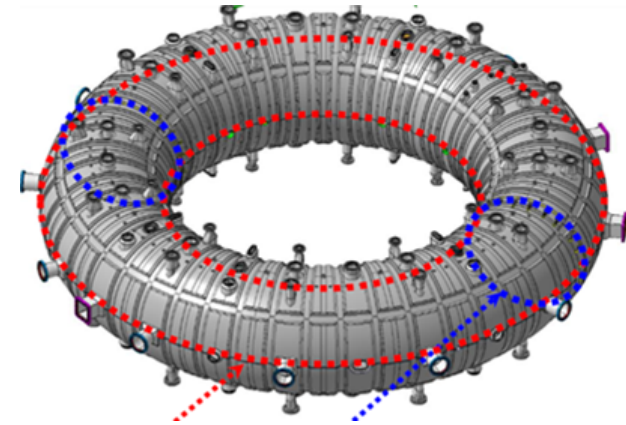


SPARC (CFS, Inc.)

$R=1.85\text{m}$, $A=3.2$
 $B_T=12.2\text{T}$, $I_p=8.7\text{MA}$

$Q > 2$ short pulse
Long-leg divertor

P.Rodríguez -Fernandez
OV/P-856



RFX-mod2 (IT)

$R=2\text{m}$, $A=4.1$
 $I_p=2\text{MA}$

Closer shell, double
poloidal gaps,
improved PFCs

L. Marrelli EX/P-1077

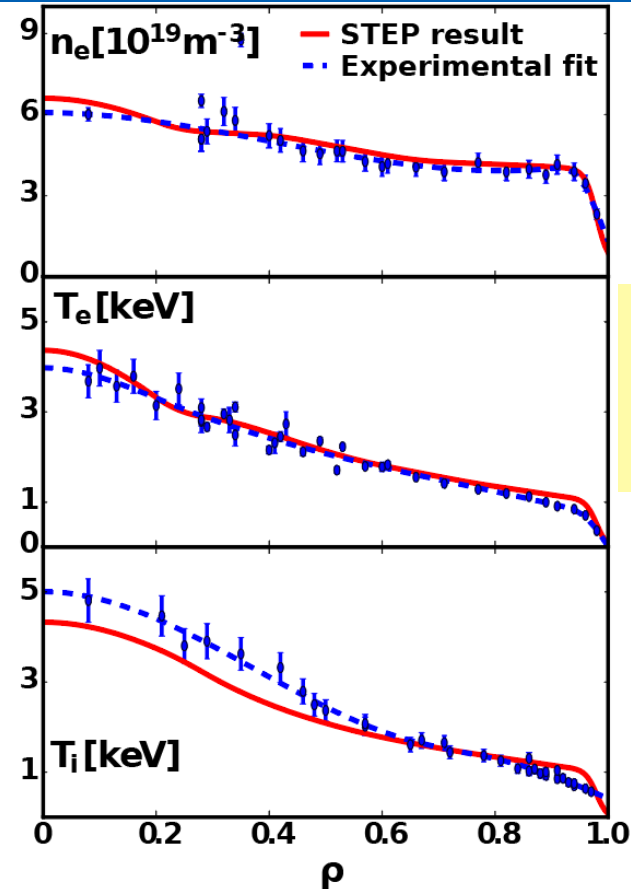
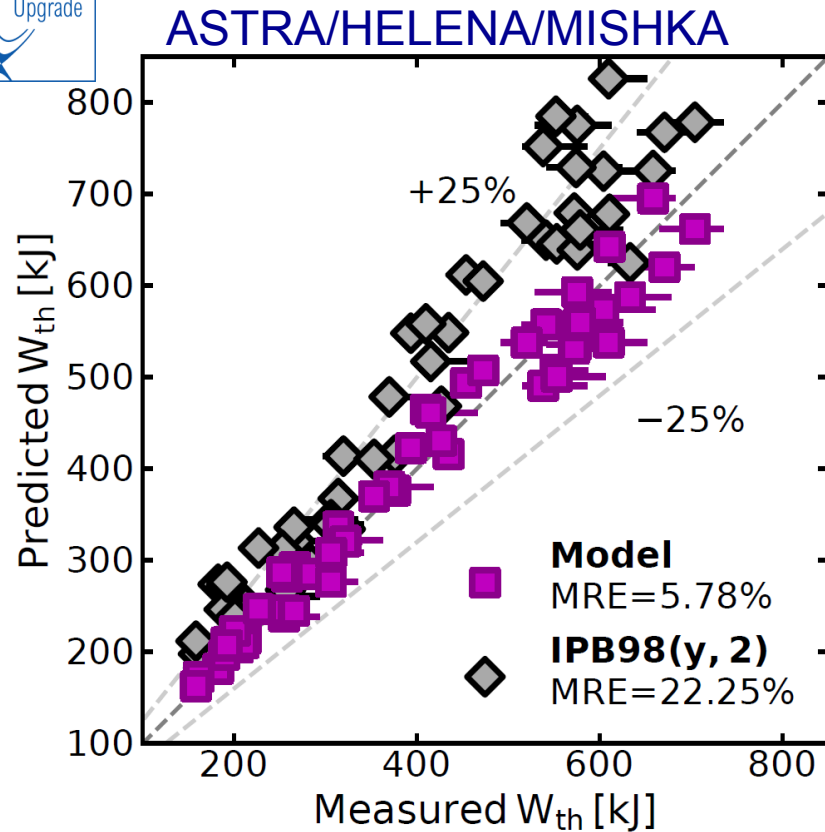
Core Confinement

- **Predict-First Modeling**
- **Impact of fast ions**
- **Isotope scaling**
- **Stellarator transport & confinement**
- **High performance in JET**
- **ST confinement**

Accurate Predict-First Models Developed



Ding EX/1-3;
J.McClenaghan
TH/P8-1016



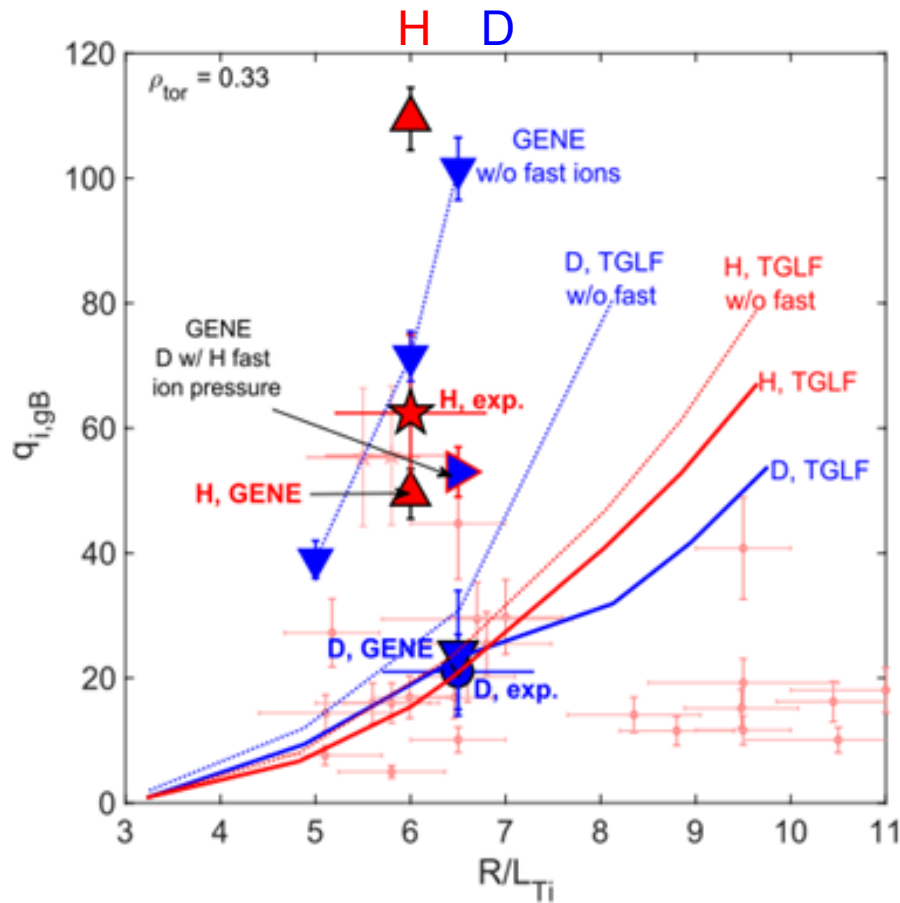
- Separatrix parameters from empirical model of gas puff & 2-pt model
- Pedestal from PB-stability & critical temperature gradient model
- Core plasma inside pedestal using TGLF
- **More accurate than scaling laws for AUG!**

- Pedestal from EPED
- Core transport from TGYRO, TGLF, NEO
- NBI and RF sources
- Time evolution from ONETWO
- **Successfully designed high β_p scenarios**

U. Stroth OV2-2; G.Tardini TH/P2-926

See also J.Citrin TH/3-2 QuaLiKiz

Impact of Fast Ions on Turbulent Transport Can Differ Between D & H



N. Bonanomi *et al*, NF 2019

J.Mailloux OV/1-2
A.Di Siena TH/4-1

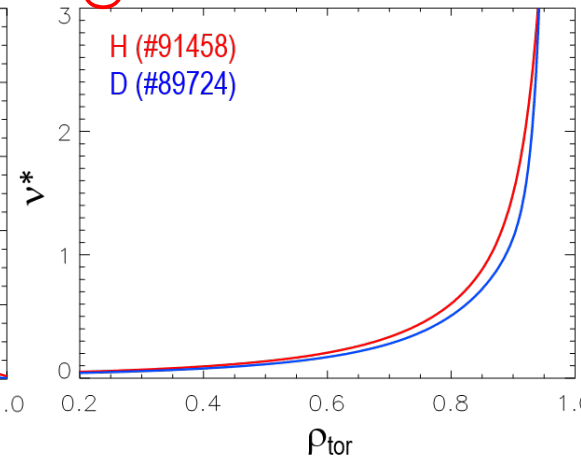
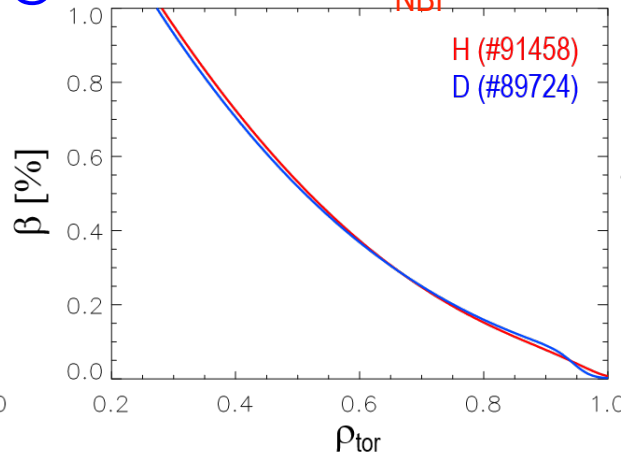
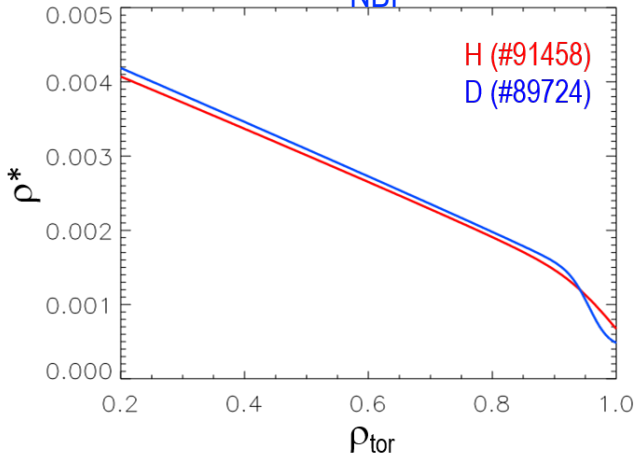
- FI impact studied in JET **D** and **H** L-mode by varying ICH ^3He resonance
- Fast ion (FI) stabilization of turbulence can produce isotope effects can be large in regimes with high Fast Ion content, beta and rotation [J. Garcia, NF 2018].
- Isotope mass differences affects FI pressure gradient via:
 - Heating deposition profile
 - FI slowing down time
- GENE (GK) modelling shows that **differences in FI in H vs D lead to strong deviations from GB scaling of thermal core transport**

Dimensionless Identity Isotope Effect Experiments

L-mode

D: (3.0T/2.5MA)
 $P_{\text{NBI}} = 6.24 \text{ MW}$ @ 82 – 91 keV

H: (1.74T/1.44MA)
 $P_{\text{NBI}} = 2.56 \text{ MW}$ @ 64 – 71 keV



Isotope: pulse#	H: #91458	D: #89724
$\Omega_i \tau_{E,th} [\text{T s}]$	0.27	0.28

$\Omega_i \tau_{E,th}$ identical in H and D

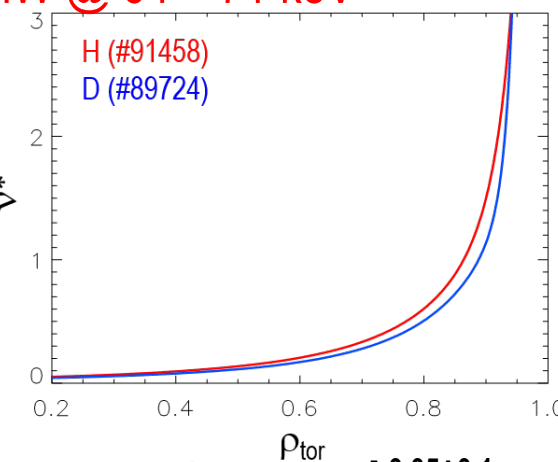
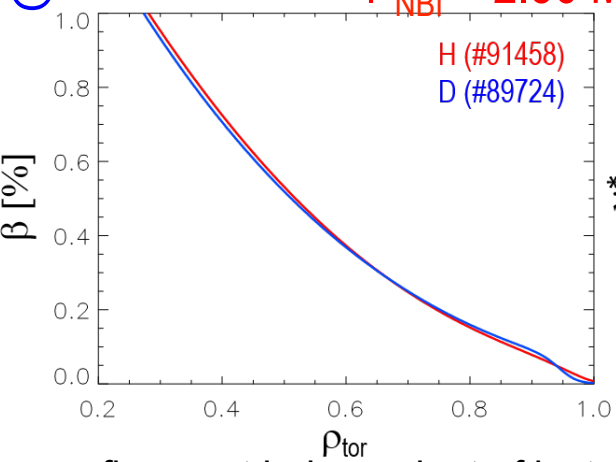
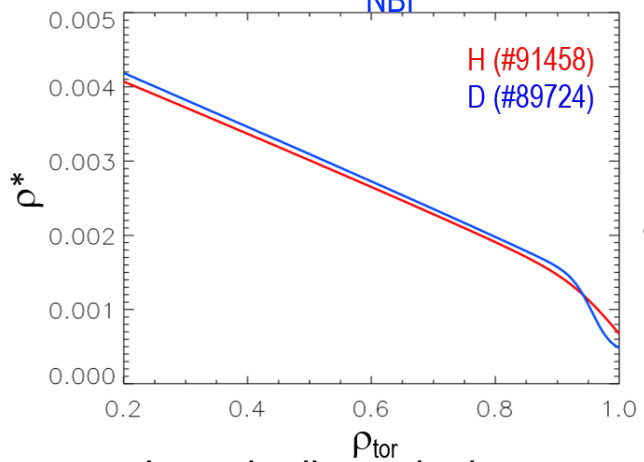
L-mode dimensionless energy confinement independent of isotope mass: $\Omega_i \tau_{E,th} \sim A^{0.05 \pm 0.1}$
 where Ω_i is the ion cyclotron frequency.

Dimensionless Isotope Effect Experiments

L-mode

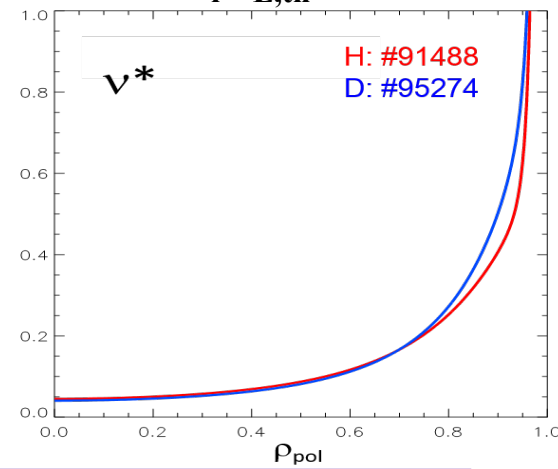
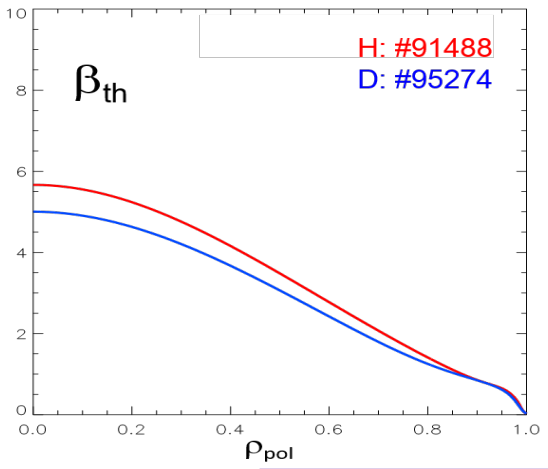
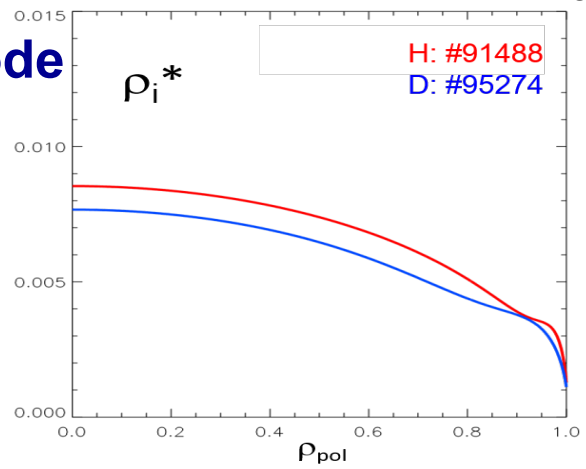
D: (3.0T/2.5MA)
 $P_{NBI} = 6.24 \text{ MW} @ 82 - 91 \text{ keV}$

H: (1.74T/1.44MA)
 $P_{NBI} = 2.56 \text{ MW} @ 64 - 71 \text{ keV}$



L-mode dimensionless energy confinement independent of isotope mass: $\Omega_i \tau_{E,th} \sim A^{0.05 \pm 0.1}$

H-mode



$\Omega_i \tau_{E,th} \text{ [T s]}$	0.105	0.15
--------------------------------------	--------------	-------------

$\Omega_i \tau_{E,th} \sim A^{0.51}$ **H-mode**
 Difference identified as coming from pedestal

Stellarator Isotope Scaling

LHD

- Database of H and D plasmas at fixed magnetic configuration (R=3.6m)
- NBI heated, dominantly heating electrons

$$P_e/P_i = 3.9 \pm 2.0$$

$$T_e(0)/T_i(0) = 1.79 \pm 0.37$$

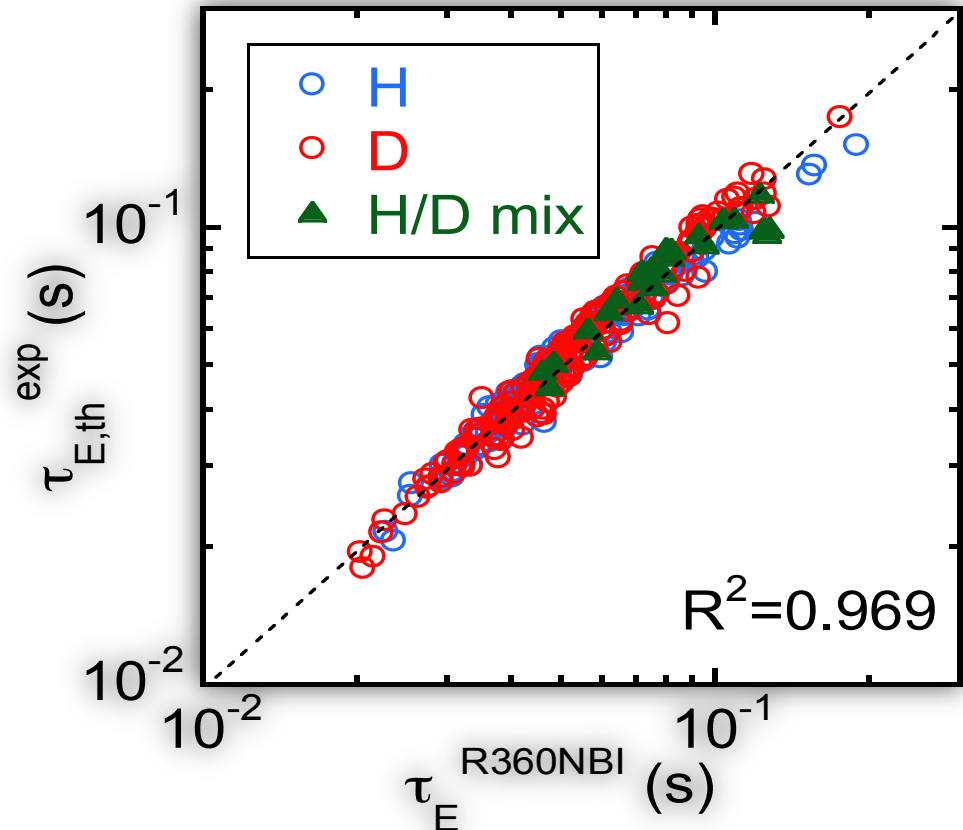
- Fit to operational parameters

$$\tau_{E,th}^{R360NBI} \propto M^{-0.07 \pm 0.01} B^{0.85 \pm 0.01} n_e^{-0.73 \pm 0.01} P_{abs}^{-0.81 \pm 0.01}$$

- Fit to dimensionless parameters

$$\tau_{E,th}^{R360NBI} \Omega_i \propto M^{0.94} \rho^{*-3.02} \nu^{*0.15} \beta^{-0.23}$$

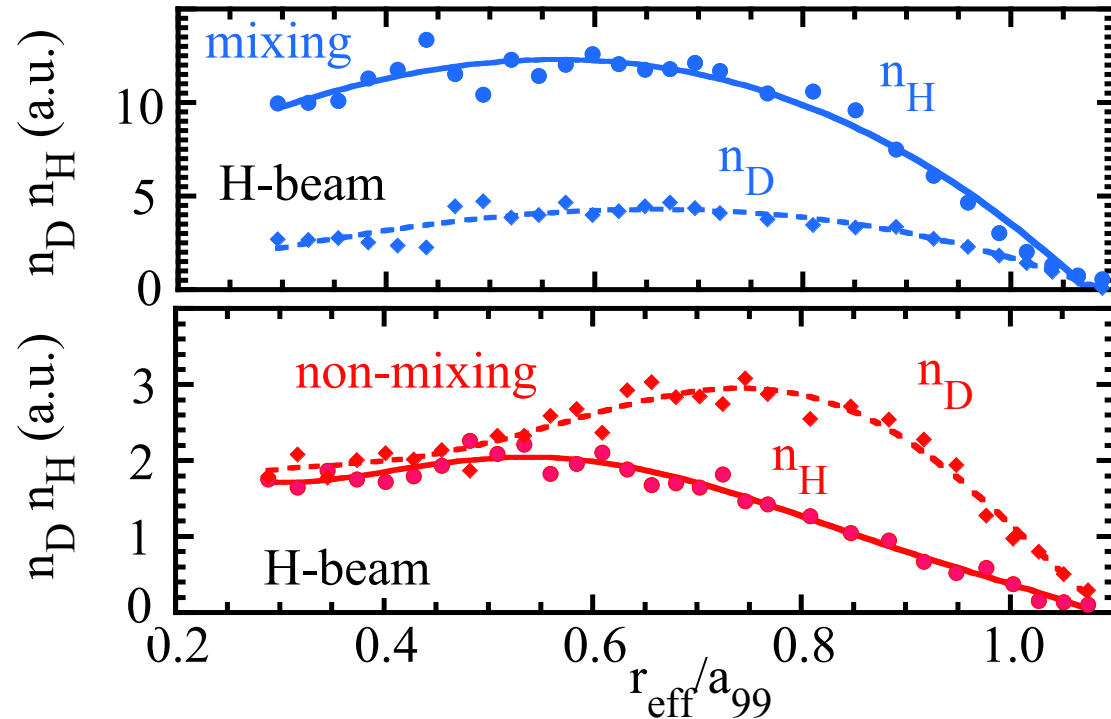
gyro-Bohm with a separate Mass-dependence



Isotope Mixing and Non-Mixing

LHD

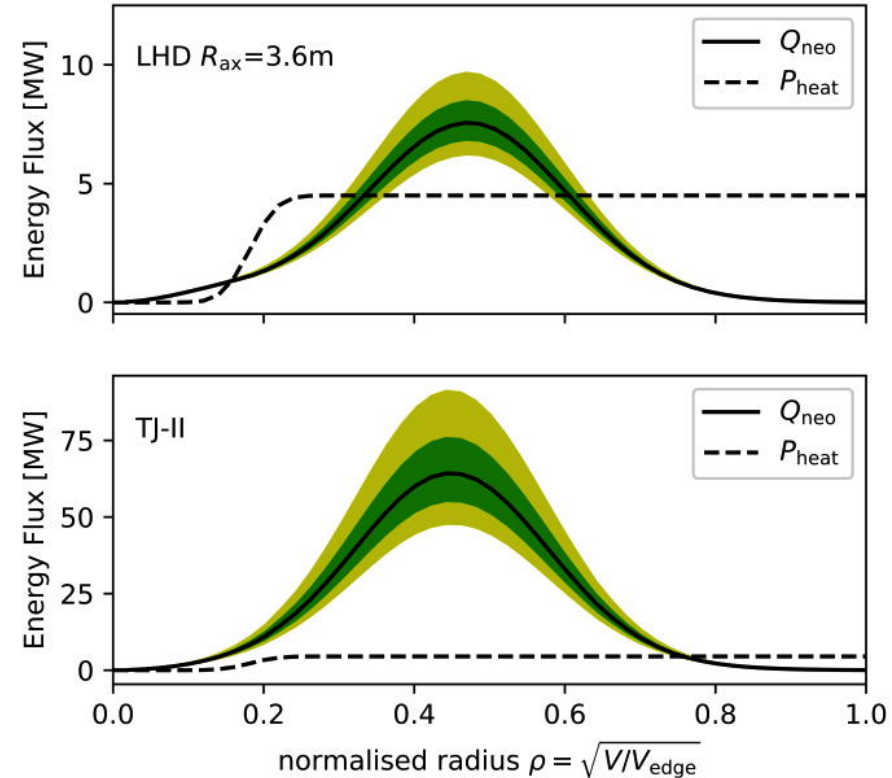
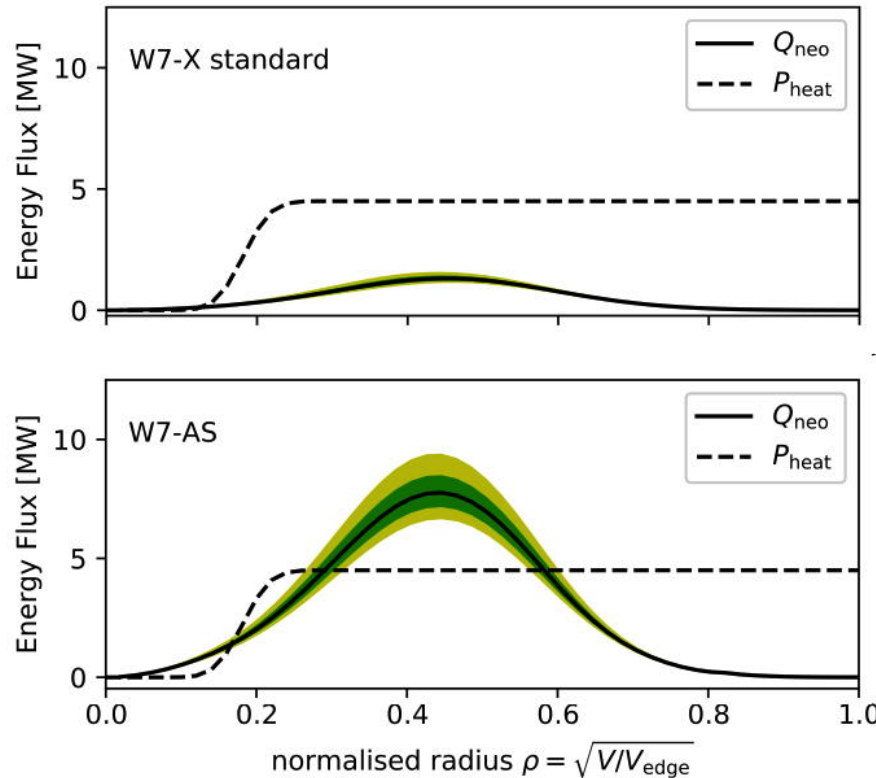
- Isotopic densities measured by bulk ion charge-exchange recombination.
- Mixing plasmas have $n_e > 2-3 \times 10^{19} \text{ m}^{-3}$, hollow density profile
- Non-mixing plasmas have low density $n_e < 2-3 \times 10^{19} \text{ m}^{-3}$, peaked density profile



- Gyrokinetic analysis suggests strong correlation with ITG-TEM
 - Mixing: core **ITG unstable**, TEM stable ($\rho = 0.5$)
 - Non-mixing: core ITG stable, **TEM unstable**

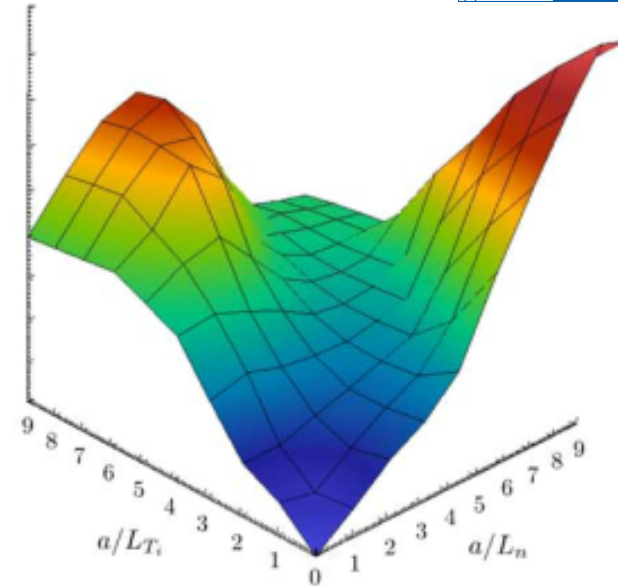
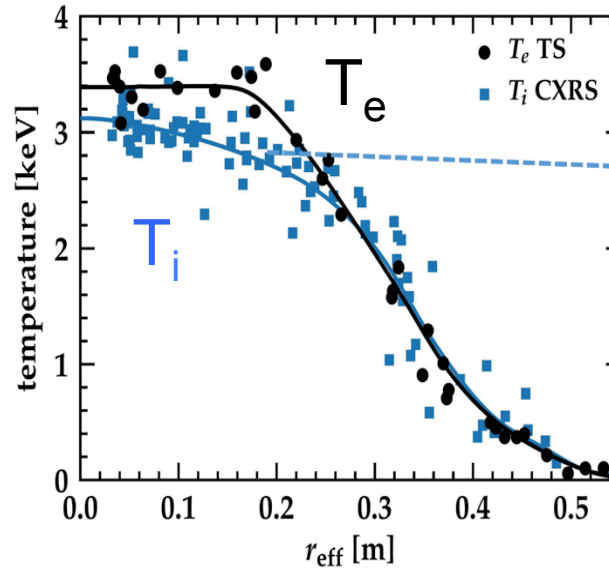
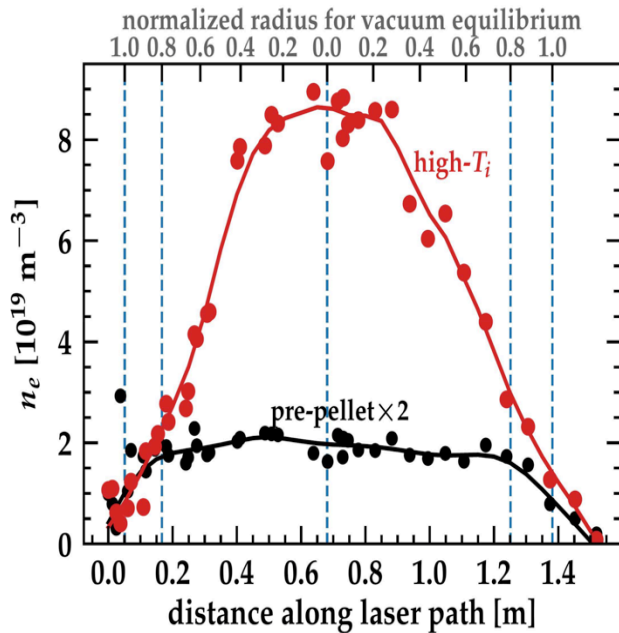
W7X: Neoclassical Optimization Successful

Calculated neoclassical energy transport for W7X profiles in other stellarator shapes



- Pellet peaked density profile to reduce ITG
- Other configurations scaled to same volume and $B=2.5\text{T}$ as W7X
- Neoclassical losses calculated using W7X density and temperature profiles
- Other configurations: losses exceed W7X heating power => temperature inaccessible!

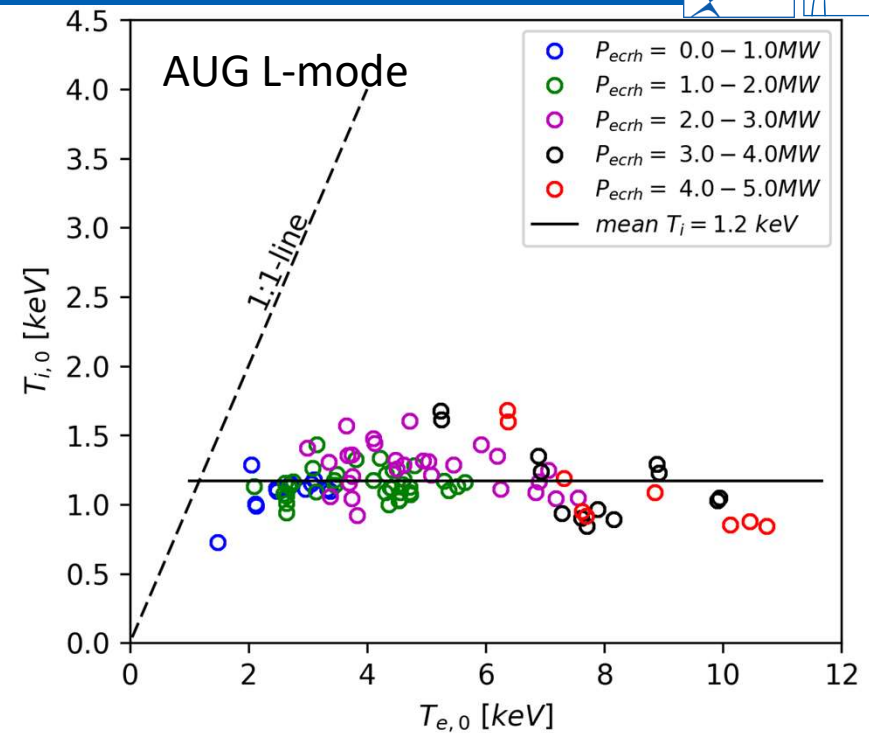
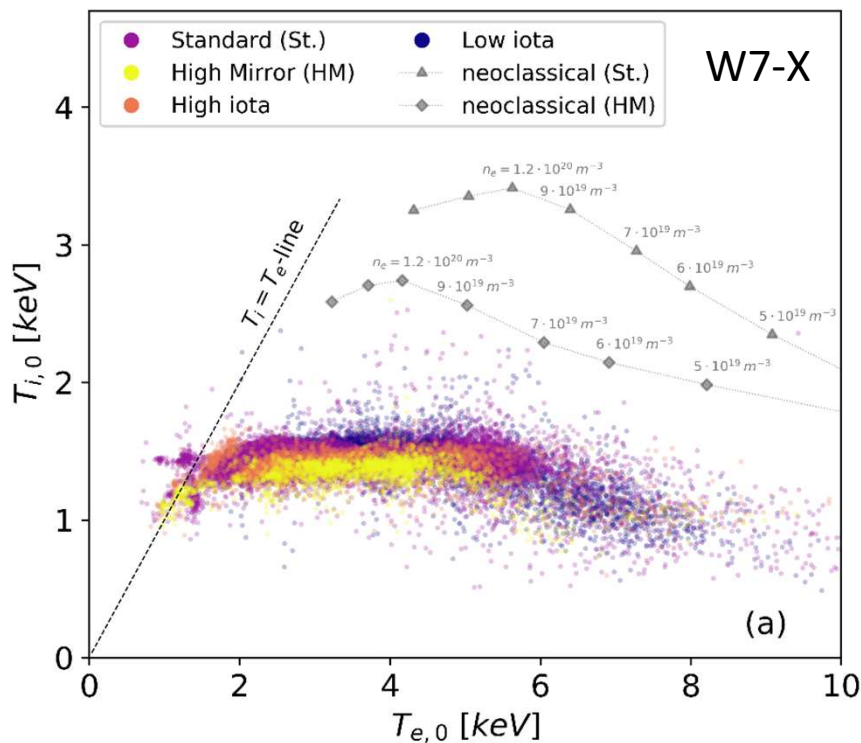
W7X: Highest Performance with Pellets



Growth rate vs density and temperature scale lengths

- ECH heating only, 4.9 MW, B=2.5T
- From GENE calculations, need $a/L_n \sim a/L_{T_i}$ to suppress ITG & TEM
- Confinement enhancement of 1.3 x ISS04 scaling
- Accessible using multi-pellet fueling
- Highest $n(0) T_i(0) \tau_E$ for a stellarator

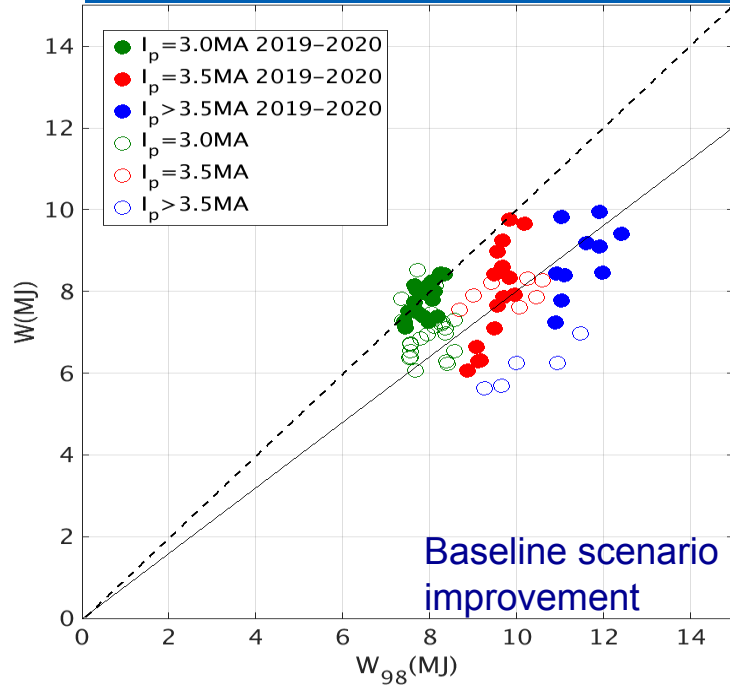
W7X and AUG see $T_i \sim 1.5\text{keV}$ clamping for gas-fueled ECH L-mode



- T_i clamps with only electron heating, independent of magnetic configuration
- ITG stronger for $T_e > T_i$ enforces marginal stability
Very difficult to increase T_i from an initial condition of $T_e \gg T_i$
- Ion-electron thermalization $\sim (T_e - T_i)/T_e^{3/2}$ weakens as T_e increases
- Enhanced confinement usually requires ITG suppression or weakening (ETB, ITB)

JET: High Performance for DT Baseline and Hybrid Scenarios

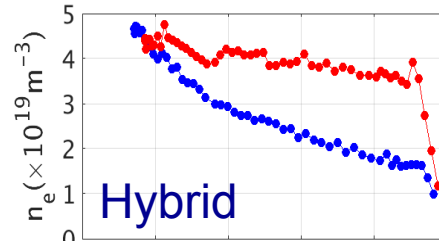
JET



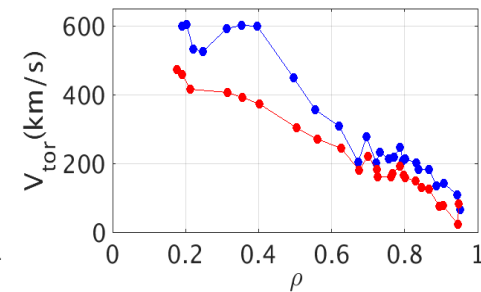
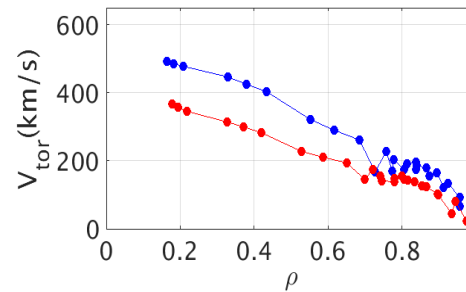
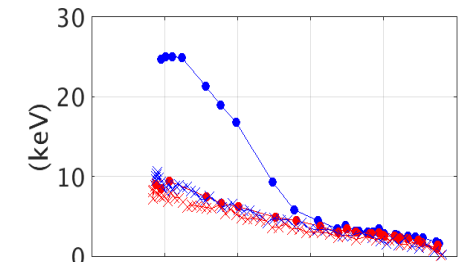
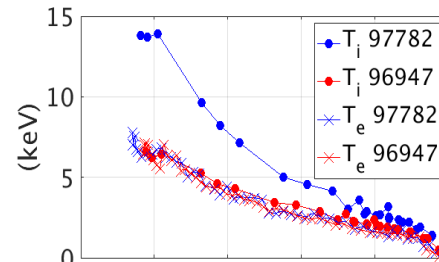
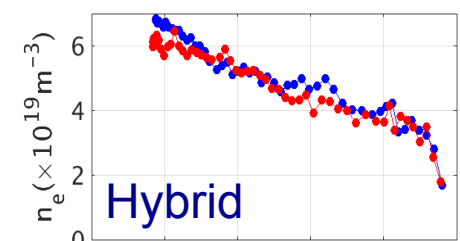
Ion transport reduced by:

- Edge impurity dilution (reducing n_i)
- Reduced gas puff + pellets (incl. Ne)
- $T_i / T_e \sim 1.6$ including pedestal top
- Strong ExB shear
- Strong rotation to centrifuge W & Ni
- Core P_{rad} stable
- Pedestal collisionality approaching ITER

Gas fuelled
H-mode entry



New low gas
ELM-free entry



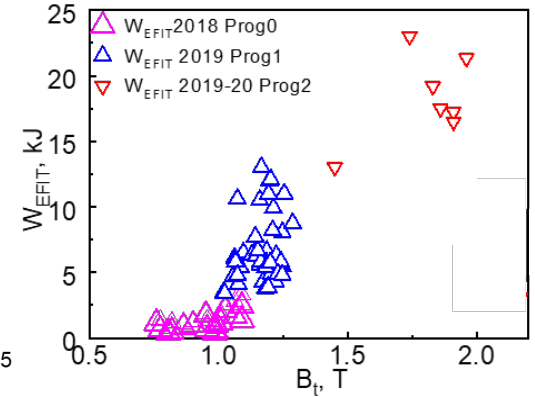
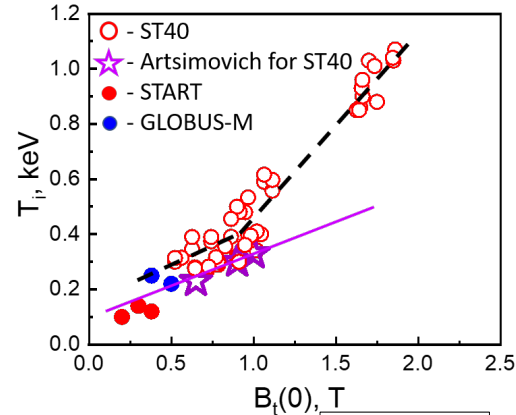
- Low-gas puff, ELM-free initial period
- $T_i > T_e$ including pedestal
- Increased rotation
- Core P_{rad} stable
- Record peak and average DD reaction rate

Spherical Torus Confinement Advances

ST-40

Sharp increase in confinement for $B_T > 1T$

M.Gryaznevich OV/4-5.4

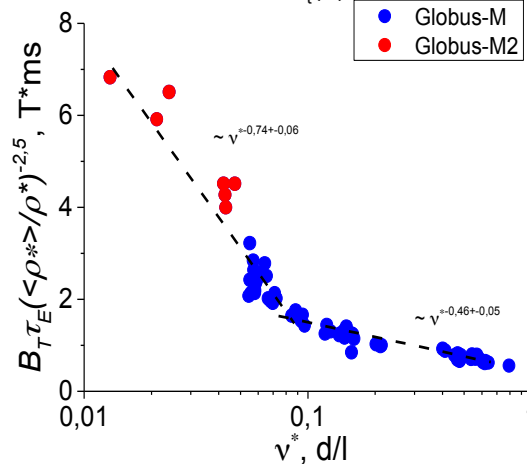


GLOBUS-M2

Extended B_T to 0.8T, I_p to 0.4MA

$B_T \tau_E \sim \nu_*^{-0.74}$ extended to lower ν_*

Yu.Petrov OV/4-5.3

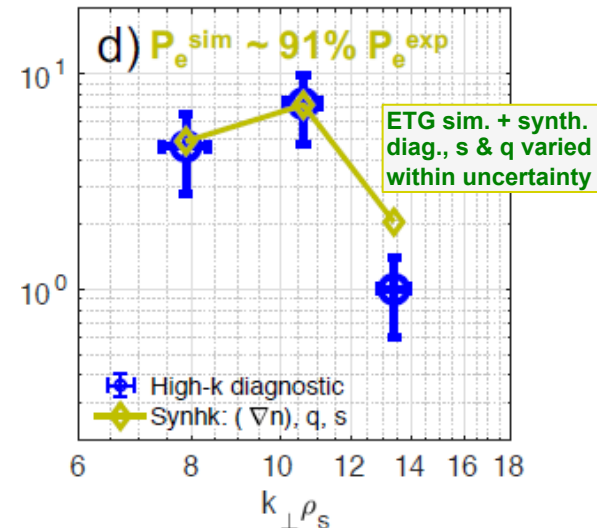


- Consistent with previous ST studies
- Not like IPB98(y,2)

NSTX-U

- Using novel synthetic diagnostic, nonlinear gyrokinetic simulations (GYRO) reproduce electron transport & high-k microwave scattering spectra for moderate- β NSTX H-mode
- Parameter scans (∇n , ∇T , q , s) used to quantify sensitivity of predicted fluxes and synthetic high-k spectra

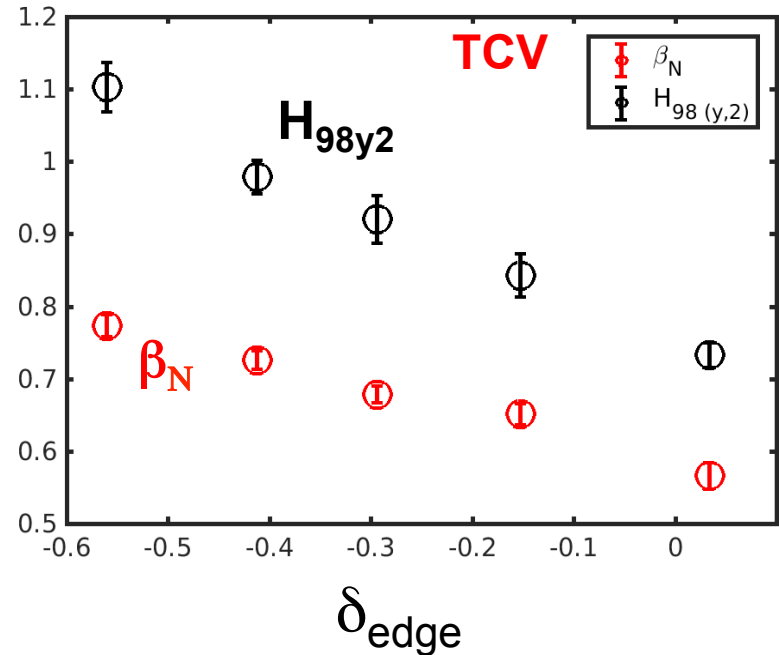
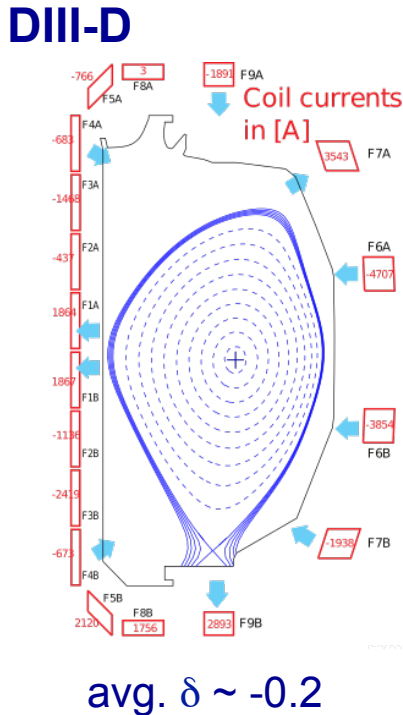
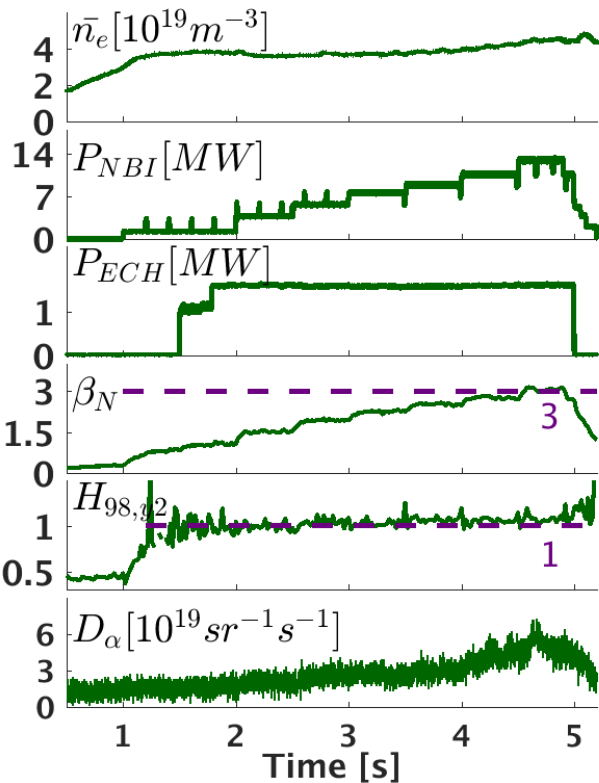
W.Guttenfelder OV/4-5.2



MHD, Stability, and Fast Ion Transport

- **Shaping: Reversed Triangularity**
- **Quasi-Symmetric Magnetic perturbations**
- **Magnetic flux pumping**
- **Fast Ion Instabilities & Transport**

Diverted Negative Triangularity Is Advantageous (TCV, DIII-D)



- $H(98y,2) \sim 1$, $\beta_N=3$, without power threshold
- L-mode edge maintained. H-mode threshold drastically higher.
- SOL heat-flux width $\sim 1.5 \times$ H-mode width
- $\tau_P \sim \tau_E$ from laser blow-off

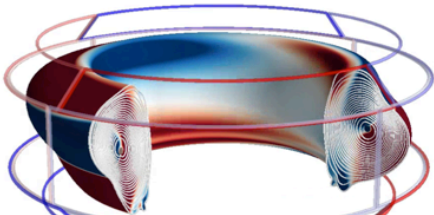
- Energy confinement improves for more negative triangularity, linearly
- Observed for OH, ECH, NBI heating
- Improvement maintained for $q_{95} < 3$, upto $\beta_N=3$
- Density fluctuations reduced inside LCFS
- Reduced SOL turbulence on low-field side, due to shorter connection length

Quasi-Symmetric Magnetic Perturbations (QSMP)

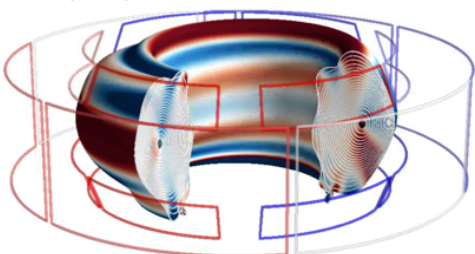
- QSMP in a tokamak: 3D magnetic perturbation that induces the minimum neoclassical 3D torque (NTV) and transport. Compared to RMP (resonant MP) or NRMP (non-resonant MP)
- Optimization for QS perturbation uses self-consistent torque response matrix
- QSMPs do not show confinement degradation in high- β flattop, or impact on L-H transition power in KSTAR and DIII-D, despite large amplitude perturbations
- Thus: Error fields can be modified towards quasi-symmetry, minimizing resonant and non-resonant effects, and minimizing confinement impact.

QSMP configuration, with large δB but minimum impact on 3D transport

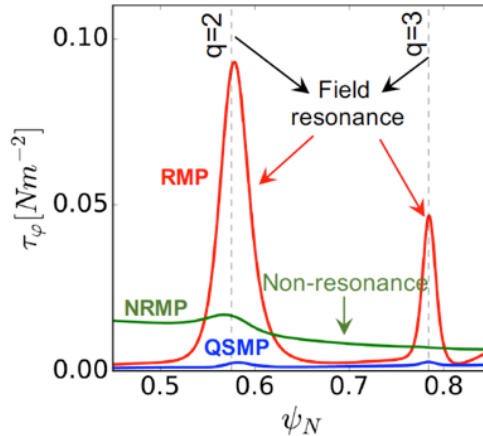
KSTAR (x25)



DIII-D (x10)

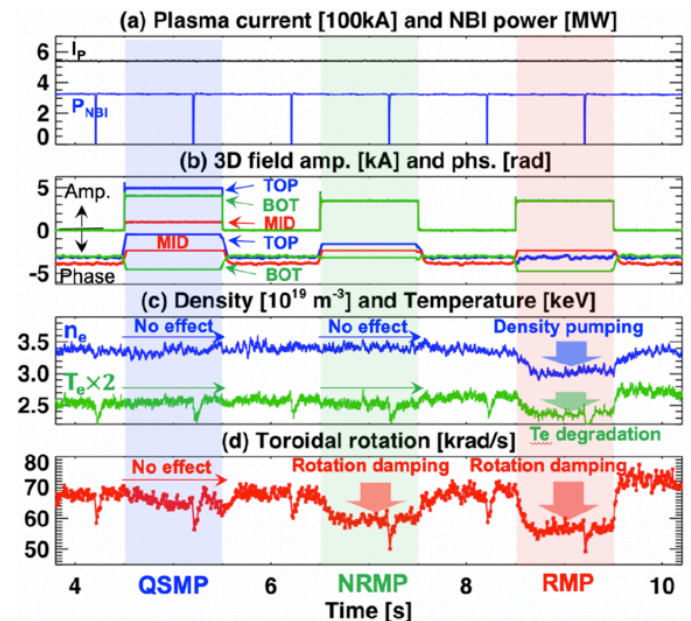


NTV prediction for QSMP, NRMP, and RMP (KSTAR example)



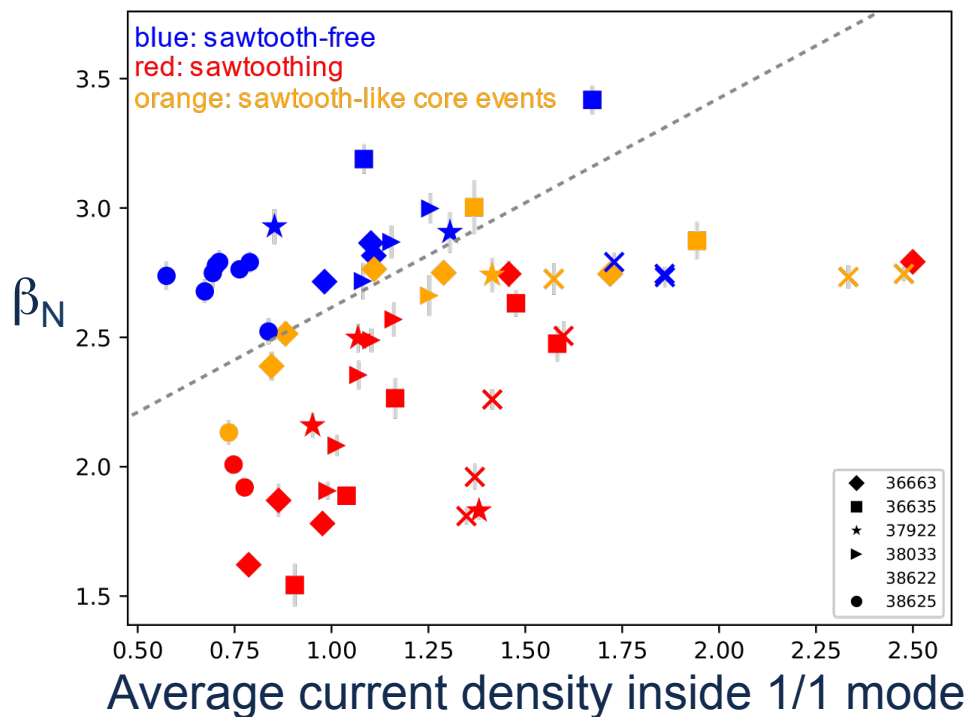
J-K Park EX/4-3

Experimental Comparison (KSTAR example)



Experimental Evidence of Magnetic Pumping at AUG

- Experimentally test new theoretical model of flux pumping at high β with (1/1) mode [I. Krebs, PoP 2017]
- Possible way to reduce needed current drive in reactors
- Cases where q-profile evolution does follow neoclassical current diffusion
- Or, central co-ECCD cannot drive $q(0)$ down, below $q=1$ (IMSE measurements, without sawteeth)
- Stronger effect at high β (like theory)
- At high non-inductive current, effect may not be strong enough to keep $q(0)=1$
- Qualitative agreement with theory, but model gives more peaked current than measurements.



Scenario prepared to assess α -driven instabilities in JET-DT

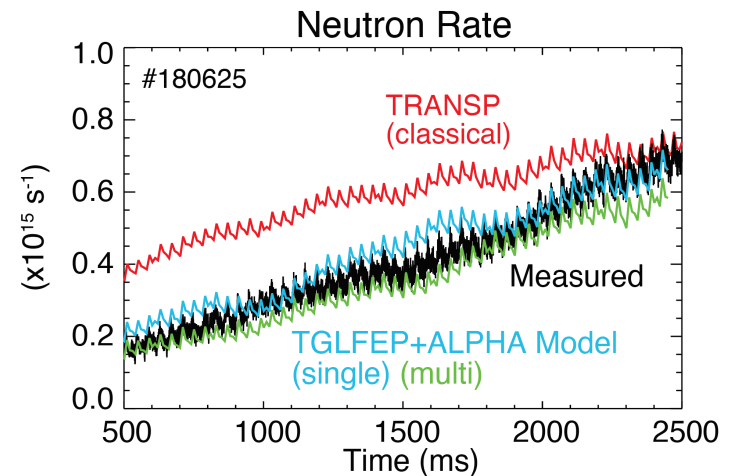
JET

- α -driven instabilities are potentially an issue for burning plasmas, including ITER. Unambiguously identified only in TFTR-DT plasmas so far.
- A dedicated scenario was developed and tested to observe α -Toroidal Alfvén Eigenmodes (TAE) in JET-DT, including:
 - Good fusion performance from Internal Transport Barrier
 - Elevated central q-profile, to lower threshold
 - Real-time control trigger to switch to afterglow at peak performance
 - NBI-only before afterglow, to not generate other fast ions
 - ELM pacing by pellets
 - Core-localised TAEs when ICRH heating used (as test)
- Extrapolations to DT using integrated modeling (TRANSP & CRONOS) predict $\beta_{\alpha}(0) \sim 0.15\%$ and ~ 9 MW of fusion power. This is larger than extrapolations for previous JET pulses, and than the TFTR-DT α -instability experiments.
- JET / TFTR comparisons included in plans for coming JET DT campaign

Control of Fast-Ion Alfvénic Modes in Advanced Steady-state Scenarios

- Energetic ion driven Alfvénic Eigenmodes (AE) are common in advanced scenarios with elevated q -min, causing transport of the energetic ions.
- Broadened energetic ion profile gives better control of AE stability in elevated q -min scenarios. Key factor is moving $\rho_{q\text{-min}}$ towards region of reduced $\nabla\beta_{\text{fast}}$
- In DIII-D NBI experiments, this was done by switching from central to off-axis neutral beams
 - Accessed 15% higher β_N
 - Ratio of expected to measured neutron emission increased by ~25% in flattop
- TGLF-EP + ALPHA critical gradient model reproduces energetic ion transport trends. Matches measured neutron rate within 12%>
- Provides basis for understanding how to avoid AE-induced energetic ion transport in ITER and future burning plasmas.

Improved fast-ion transport modeling



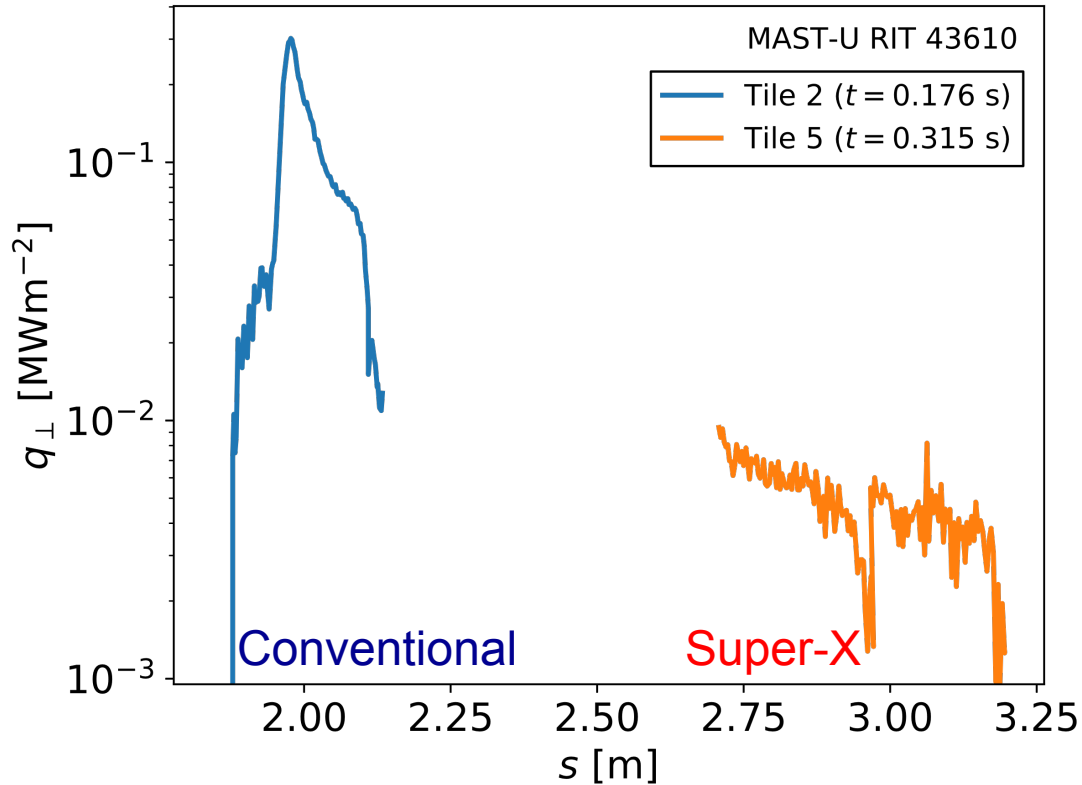
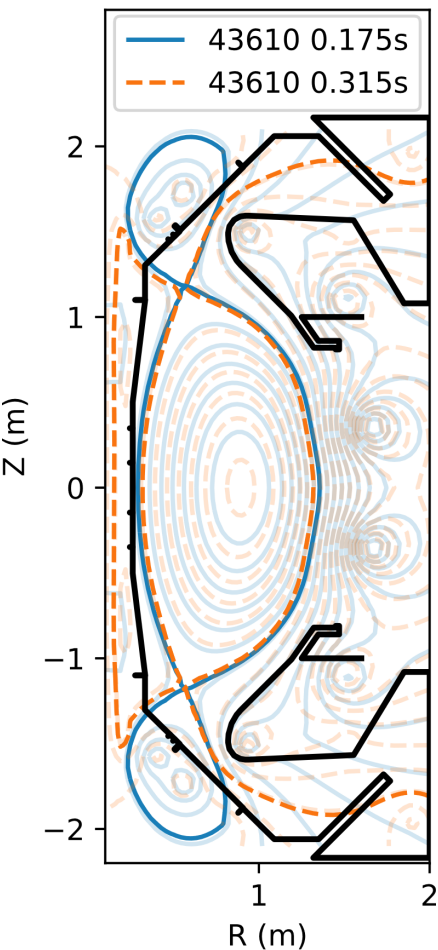
Divertor & Scrape-off-layer

- **Super-X divertors**
- **Controlled Detachment**
- **Stellarator divertors**
- **Divertor experiments and modeling**

Heat Flux Reduced in Super-X Divertor

MAST-U

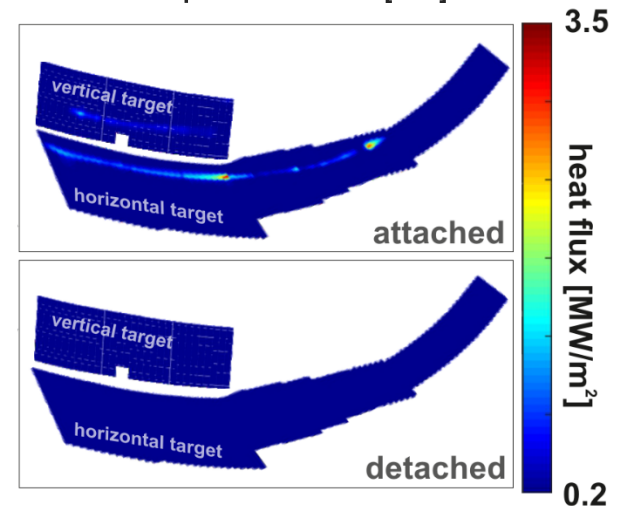
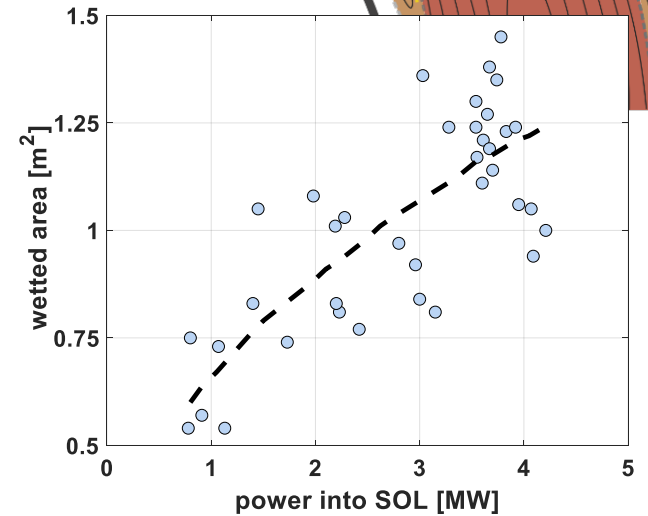
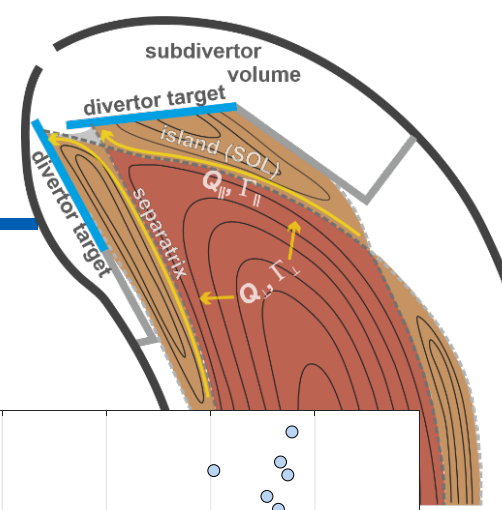
Substantial reduction in the outer divertor heat flux observed in the Super-X vs. conventional divertor



Initial studies have focused on moving the outer strike points to large major radius and reducing the poloidal field there to produce Super-X configurations.

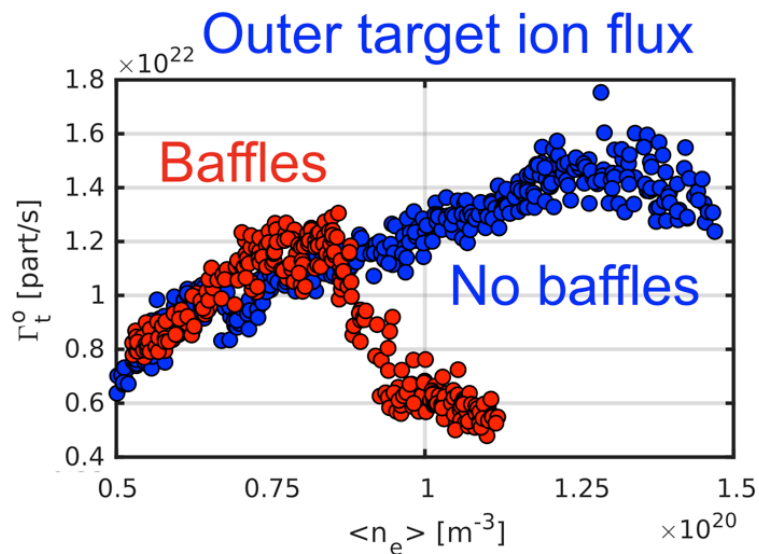
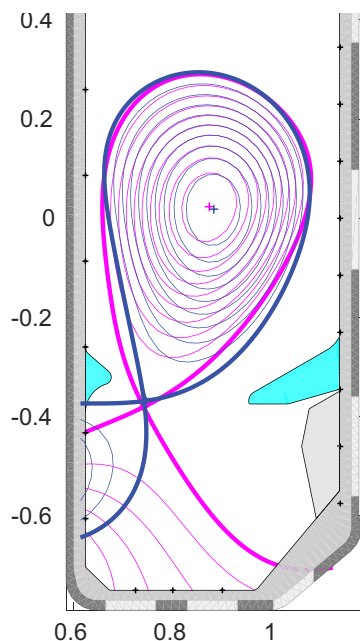
W7X Island Divertor Is Highly Effective

- Core plasma surrounded by helical island chain (typ. 5/5) that interfaces to divertor baffles.
- Wetted area up to 1.5 m² to spread exhaust heat, increases with P_{SOL}
- Islands shield against impurity sources, e.g. hot spots on divertor tile edges
- Stable, complete detachment in many scenarios achieved, for up to 26 sec. Detachment density $\sim 10^{20} \text{ m}^{-3}$
- Below detachment, observe high recycling regime, enabled by counter-streaming flows in islands.

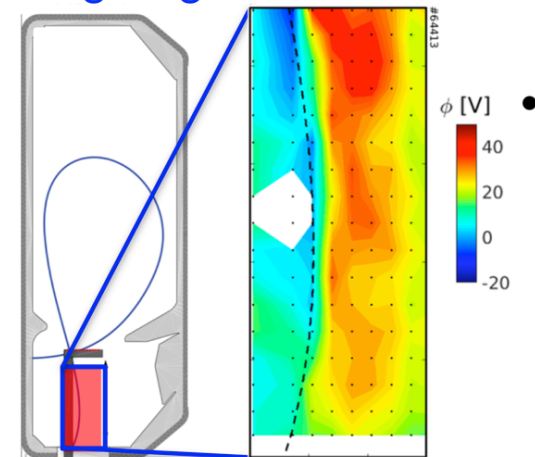


EPFL TCV with Baffles – a Divertor Testbed

- Divertor baffles increase neutral pressure $\sim 5x$, increase divertor dissipation. Facilitates detachment in L- and H-mode.
- Detachment density $\sim 25\%$ lower with baffles
- Flexible coil-set enables divertor leg steering
- SOLPS drift simulations predicts key features and trends. E.g, potential structure, currents.
- Reduction of detachment threshold for Super-X (large radius target) lower than originally predicted with baffles. May be due to details of geometry.

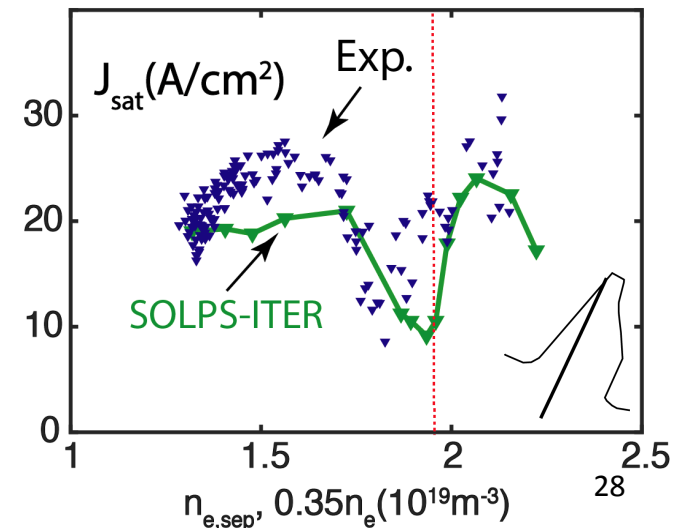
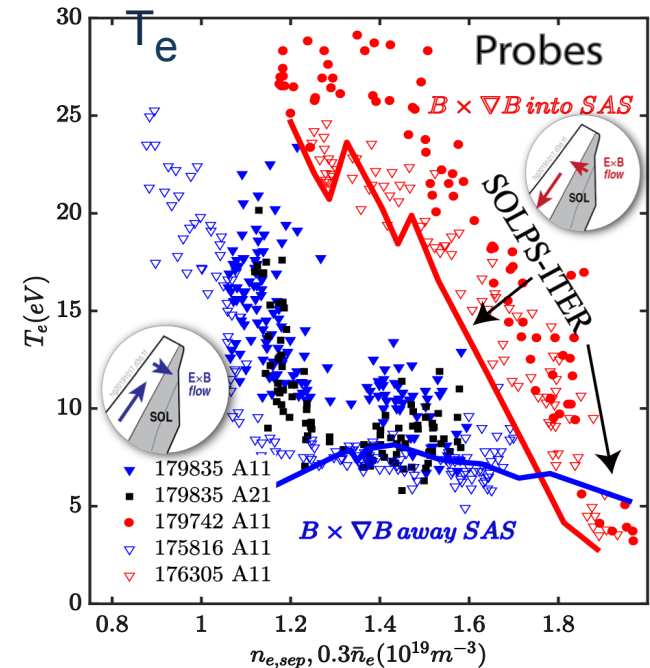
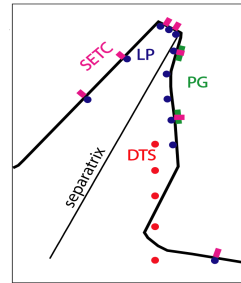


Measured V_{pl} with predicted neg. region in Rev. B



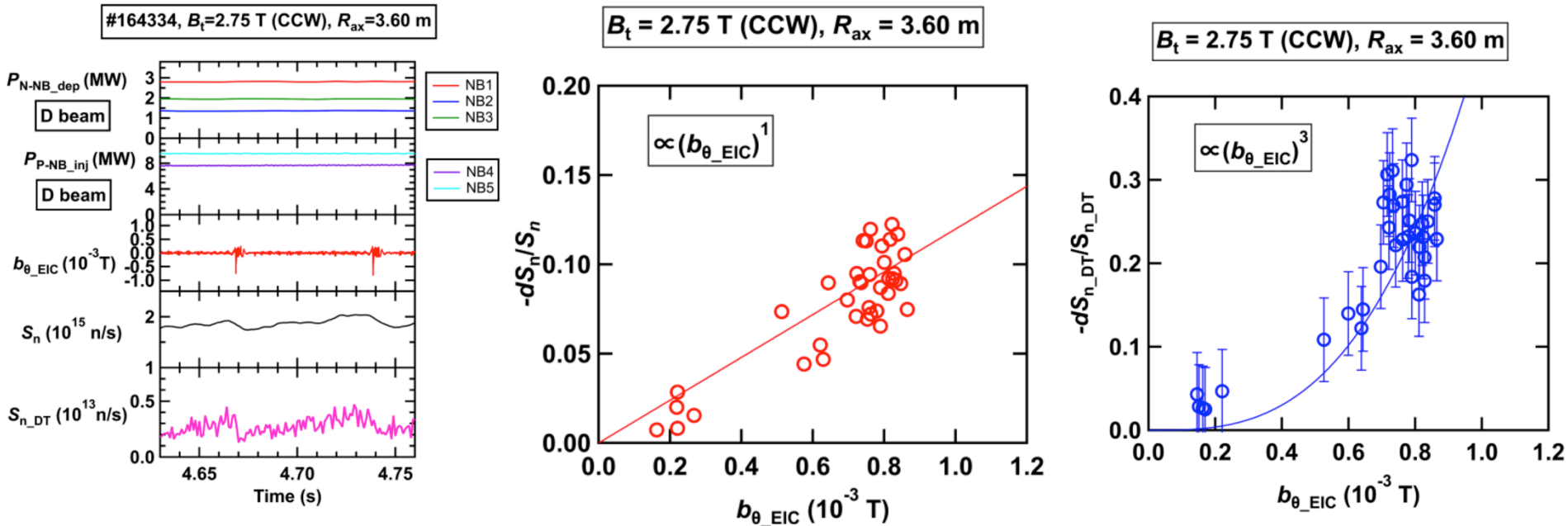
DIII-D SAS is a Divertor Testbed

- SAS: Small Angle Slot divertor
- Interaction between drift flows and divertor geometry has important effects on dissipation
- SOLPS-ITER with drifts reproduces trends found in experiments
 - Lower T_e and detachment density with drift away from divertor.
 - Drifts are comparable to geometry in effects on recycling flux and neutral density
- Experiment and modeling both found that geometry+drift can alter variation of dissipation
 - Including T_e bifurcation and J_{sat} reduction



Thank You

A Comprehensive Study of Energetic Particle Transport due to Energetic Particle Driven MHD Instabilities in LHD Deuterium Plasmas



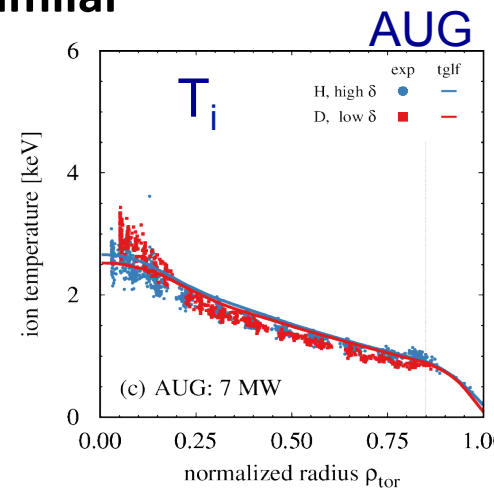
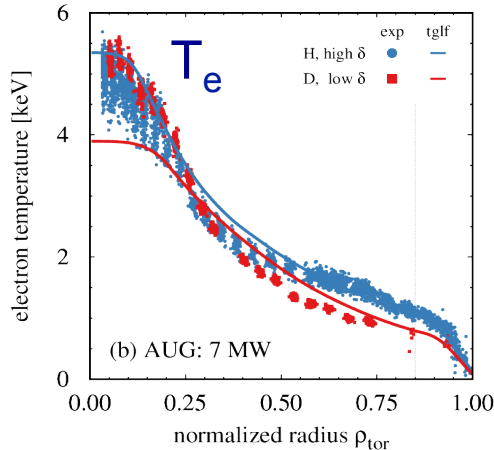
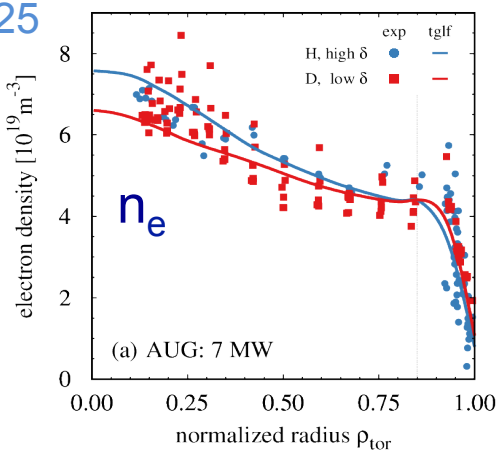
- Beam ion and DD fusion born triton transport due to energetic-particle-driven MHD instabilities (EIC) is simultaneously studied in the Large Helical Device (LHD).
- Drop of total neutron emission rate (S_n) by EIC shows enhanced beam ion transport due to EIC.
 - Experiments in full D and H/D beam conditions shows that EIC induces up to 8% of passing transit beam ion losses and up to 60% of helically-trapped beam ion losses.
- Drop of secondary DT neutron emission rate (S_{n_DT}) increases substantially with the EIC amplitude to the third power and reaches $\sim 30\%$.
 - 1 MeV tritons are largely transported because the tritons are barely confined in LHD.

Dimensionless-identity comparisons Controlled Pedestal Height (AUG, JET)

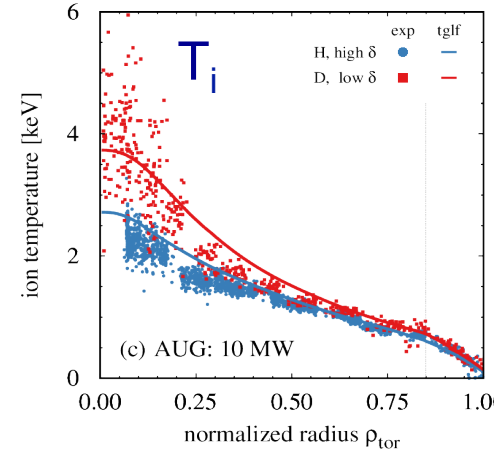
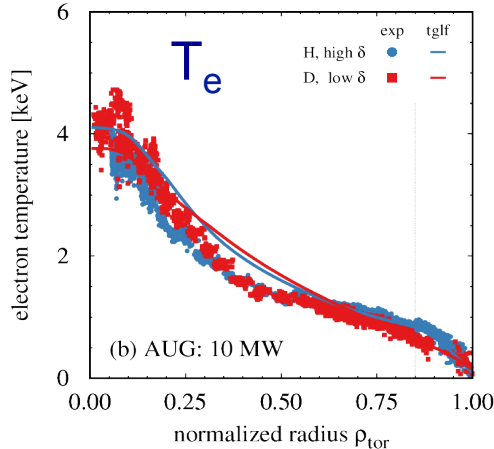
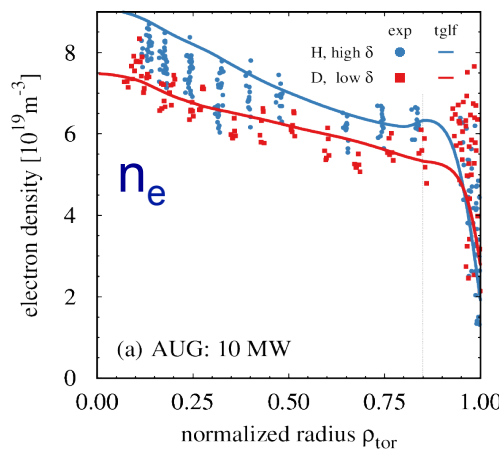
Matched edge profiles by adjusting δ , keeping source profiles similar

H: $\delta=0.37$ D: $\delta=0.25$

Low NBI power:
core profiles
similar, good
agreement with
TGLF



High NBI power:
 T_i higher in D =>
reduced ion heat
Transport



- Nonlinear GENE simulations: higher fast ions pressure in D-plasmas stabilizes turbulence (slowing-down time)
- Similar experiments in JET